# Electron Energy Loss and DFT/SCI Study of the Singlet and Triplet Excited States of Aminobenzonitriles and Benzoquinuclidines: Role of the Amino Group Twist Angle

**Christophe Bulliard, Michael Allan,*,† Gabriele Wirtz, and Edwin Haselbach**
*Institut de Chimie Physique, Université de Fribourg, Pérolles, CH-1700 Fribourg, Switzerland*

**Klaas A. Zachariasse**
*Max-Planck-Institut für biophysikalische Chemie, Abteilung Spektroskopie und Photochemische Kinetik, D-37070 Göttingen, Germany*

**Norbert Detzer**
*Institut für Physikalische Chemie, Universität Mainz, Jakob Weldel Weg 11, D-55099 Mainz, Germany*

**Stefan Grimme*,‡**
*Institut für Physikalische und Theoretische Chemie der Universität Bonn, Wegelerstrasse 12, D-53115 Bonn, Germany*

*Received: March 17, 1999; In Final Form: June 2, 1999*

Spectroscopic consequences of varying the twist angle of the amino group in aminobenzonitrile systems in the electronic ground state are investigated by applying electron energy loss (EEL) spectroscopy and density functional theory to 4-*N*,*N*-dimethylaminobenzonitrile (DMABN), 4-*N*,*N*-dimethylamino-3,5-dimethylbenzonitrile (MMD), benzoquinuclidine (BQ), and 6-cyanobenzoquinuclidine (CBQ). A number of singlet and triplet excited states was observed and assigned with the help of DFT/SCI theory. The results characterize the gas-phase spectroscopy of the molecules and verify to within 0.3 eV the predictive power of DFT/SCI theory for vertical states over a wide range of twist and pyramidalization angles. The amino group configuration in the relaxed charge-transfer state of dual fluorescent aminobenzonitriles in solution cannot be directly deduced from the present data, however.

## Introduction

The dual fluorescence of 4-*N*,*N*-dimethylaminobenzonitrile (DMABN), which exhibits an anomalously red-shifted band, was discovered by Lippert et al. 40 years ago.[1] This feature has since then been found in many molecules structurally related to DMABN and in other aromatic electron donor−acceptor systems. Dual fluorescence has not been detected in the gas phase, which indicates that solute−solvent interactions play an important role in these systems.

Grabowski and co-workers proposed that the anomalous fluorescence originates from a structurally relaxed excited state where the amino group is rotated by 90° with respect to the plane of the benzonitrile moiety, resulting in the "twisted intramolecular charge transfer" (TICT) state.[2,3] The charge-transfer (CT) character of the excited state, a common feature in all descriptions of the dual fluorescence phenomenon, is derived from the measurement of a large dipole moment of the emitting state.[3−10] The assumption of a twisted excited state (i.e., the TICT hypothesis) was based on model compounds in which the amino group is held at a specific twist angle in the ground state by a suitable molecular architecture.[3,11,12] When the original TICT hypothesis was formulated, it was assumed that DMABN had an overall planar conformation in the ground state.

Recently, it has been shown that the anomalous CT fluorescence only occurs in compounds with close-lying $S_1$ and $S_2$ states and that the change in configuration of the amino nitrogen from pyramidal toward planar is an important reaction coordinate in the intramolecular charge-transfer reaction.[13−15] In addition, the photophysical significance of the model compounds considered to support the TICT hypothesis was questioned[16] and it was shown that the correlation coefficient between the oxidation potential of the amino group and the energy of the CT state in a series of 4-aminobenzonitriles is considerably smaller than the value 1.0 required by the TICT model.[17]

In the extensive theoretical study of Serrano-Andrés et al.[14] the accurate CASPT2 method was employed. The conclusion was that (i) twisting is an essential relaxation mode to lower the energy of the excited CT state and that (ii) the proximity of the $S_1$ and $S_2$ states is necessary to promote the reaction from the Franck−Condon state reached after light absorption to the emitting CT state. It should be noted, however, that the ground-state structure of DMABN was not entirely correctly reproduced in these calculations. In particular, the bond length between the amino nitrogen and the phenyl ring[18] was overestimated, which may affect the calculated rotational barrier of this bond in the ground as well as in the excited state.

Other types of structural relaxation in the excited CT state have been proposed more recently on the basis of theoretical calculations, such as in-plane bending of the cyano group in DMABN. Such a bent state was also suggested to correspond

---

* To whom correspondence should be addressed.
† E-mail: Michael.Allan@unifr.ch.
‡ E-mail: grimme@thch.uni-bonn.de.

10.1021/jp990922s CCC: $18.00

**CHART 1**

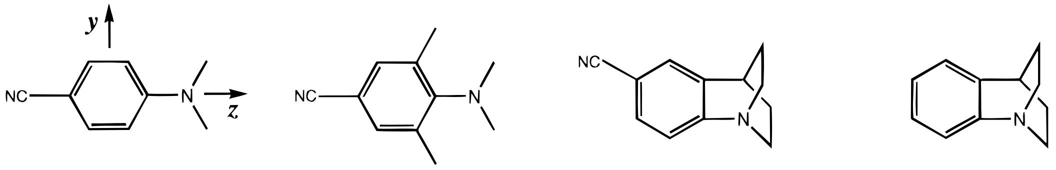

DMABN MMD CBQ BQ

to the minimum energy structure of a CT state in the related benzethynes.[15] This prediction could, however, not be corroborated experimentally.[19]

The phenomena of dual fluorescence and structural relaxation of excited states, which play an important role in photochemistry and photobiology, have been extensively investigated both experimentally and theoretically. The relevant literature has been reviewed by Rettig.[11,12] An informative overview, including a comprehensive list of earlier theoretical investigations, has been given in the paper of Serrano-Andrés et al.[14] More recent theoretical work has been cited by Scholes et al.[20] and Parusel et al.[21]

The aim of this work is to study the spectroscopic consequences of various ground-state twist angles in aminobenzonitrile systems, using the compounds 4-*N*,*N*-dimethylaminobenzonitrile (DMABN) with no twist in the electronic ground state, 4-(dimethylamino)-3,5-dimethylbenzonitrile (MMD) in which steric hindrance leads to an intermediate twist angle of 59°,[19] and 6-cyanobenzoquinuclidine (CBQ) with a fixed 90° twist angle (Chart 1). (The related problem, the effect of the ground-state twist angle on the spectroscopy of the positive ion, has been studied by Rettig and Gleiter[22] using photoelectron spectroscopy.) Benzoquinuclidine (BQ), also shown in Chart 1, has been included in the study to clarify the role of the cyano group.

Electron energy loss (EEL) spectroscopy is employed to study the excited states in the gas phase. The relaxed selection rules of this method permit the observation of the dipole and/or spin-forbidden transitions in many instances, thus providing more complete spectroscopic information than photoabsorption. The experimental study is complemented by a theoretical density functional study of both singlet and triplet excited states, including interaction between singly excited configurations (DFT/SCI). This method has been proven to be capable of predicting transition energies of fairly large molecules with high accuracy, in particular describing correctly singlet and triplet transitions of valence and Rydberg types in a consistent manner.[23−25]

## Experimental Section

The trochoidal electron spectrometer used in the present work has been described in detail previously.[26,27] It uses magnetically focused trochoidal monochromators as electron energy filters and a collision chamber with only small apertures for incident and scattered electron beams. This construction results in small sample consumption and high sensitivity, which are imperative prerequisites for recording a spectrum with a small amount of sample (ca. 50 mg). The experiment involves intercepting the sample vapor at low pressure (ca. $10^{-4}$ mbar) with a beam of electrons of varying incident energy $E_i$ and detecting electrons scattered at a fixed residual energy $E_r$. The incident electrons can excite the target molecules, thereby losing an amount of kinetic energy $\Delta E = E_i - E_r$ equal to the excitation energy. A spectrum of the excited states is obtained by plotting the scattered electron current $I_s$ against the electron energy loss $\Delta E$.

This instrument detects electrons scattered at 0° and at 180°.[26,28] At $E_r = 20$ eV the backward scattering cross section is very small and the observed spectra are due essentially to electrons scattered in the forward direction. Dipole selection rules apply to excitation by electron impact in the limit of forward scattering and high electron energies, i.e., in the limit of nearly zero momentum transfer. The residual energy of 20 eV is sufficiently high that the spectra recorded at this energy are dominated by dipole-allowed transitions. Band intensities are then indicative of the dipole oscillator strengths. However, only a qualitative comparison of EEL intensities and oscillator strengths is possible, as the present electron energy is not high enough to exclude excitation by resonances or by higher multipoles.

The cross sections for the dipole allowed transitions decrease with decreasing incident electron energy, whereas the cross sections for excitation of the triplet states generally peak at residual energies of 1−5 eV. Triplet bands are therefore prominent in the spectra recorded with low residual energies. The cross sections for excitation of the triplet states are furthermore not forward-peaked but more isotropic with respect to scattering angle; in some cases they are even strongly backward-peaked.[29] The capacity of the present instrument to detect the backward-scattered electrons is thus essential for the detection of triplet states.

We have also recorded the excitation functions of the individual excited states[30,31] but do not present them here, since they are not essential for the present discussion. These functions generally exhibit maxima due to resonances. As a consequence, the relative intensities of the individual triplet states in the energy-loss spectra vary with residual energy. We recorded the triplet spectra at various residual energies in the range 0.03−3.0 eV,[30,31] but since only the energies of the triplet states and not the details of their excitation are discussed here, we show only the sum of the spectra obtained with residual energies in the range 1−3 eV. The resolution was ca. 0.05 eV, and the energy scale is accurate to within 0.03 eV.

A commercial sample (Schuchardt/Merck) of DMABN was purified by "dry column chromatography" (DCC) according to Loev[32] (stationary phase consisting of alumina from ICN, neutral, activity 3; mobile phase consisting of cyclohexane−toluene, 1/1, toluene) and by sublimation (mp 74−75 °C). Purity was tested by thin layer chromatography (TLC) (stationary phase alumina; mobile phase cyclohexane−toluene 1/1). The synthesis and purification of MMD is described in ref 6, that of CBQ in ref 33. BQ was synthesized according to ref 34 and purified by DCC (stationary phase consisting of alumina from ICN, neutral, activity 3; mobile phase consisting of toluene and trichloromethane) and by sublimation (mp 68−69 °C). Purity was tested by TLC (stationary phase silica; mobile phase trichloromethane−methanol 9/1).

## Theory

The method for the description of excited states of closed-shell molecules using density functional calculations, combined with a single excitation configuration interaction treatment (DFT/SCI), has been developed recently.[23] It is superior to the standard ab initio HF/SCI approach because of the implicit account of dynamical electron correlation effects. The errors in the excitation energies of valence and Rydberg excited states obtained with this method were not found to exceed 0.2 eV for a wide range of molecules.[23−25]

The present DFT calculations were performed with the TURBOMOLE suite of programs.[35,36] Becke's hybrid exchange correlation functional (B3-LYP)[37] was used throughout. Valence double-$\zeta$ AO basis sets (C, N, 3s2p; H, 2s)[38] with polarization functions on the non-hydrogen atoms (VDZd, N, $\alpha_d = 1.0$; C, $\alpha_p = 0.8$) were used to optimize the ground-state structures within the symmetry constraints: $C_{2v}$ (DMABN), $C_s$ (CBQ, BQ), and $C_1$ (MMD)

The planar geometry of DMABN predicted by B3LYP/VDZd is in disagreement with experimental data where a pyramidalization angle at the dimethylamino group (12° and 15°)[18,39] was found. However, this influences the calculated spectral data only marginally as was shown in ref 21. Note that a pyramidalized DMABN geometry is obtained with a larger TZP basis set at the B3LYP level.[40]

The minimum energy structure of MMD at the DFT level has $C_2$ symmetry with a twisting angle of about 58° (no pyramidalization). Employing this structure in the DFT/SCI calculations yields incorrect results for the first (CT) band, i.e., an excitation energy that is too low and an intensity that is too high. We have thus reoptimized the geometry at the Hartree−Fock−SCF level with the VDZd basis and found a pyramidalized structure with twisting and pyramidalization angles of 76.2° and 24.2°, respectively. This geometry was used in the subsequent CI calculations of the spectrum. The optimized structure of CBQ has an amino group twist angle of 90°. Owing to the incorporation of the nitrogen atom in the bicyclic rings, the pyramidalization angle is large (57.5°) and the two bond angles $C_{Ar}-C_{Ar}-N$ deviate strongly from 120° (124° and 115°).

All computed excitation energies correspond to vertical transitions; i.e., they were obtained by employing the ground-state geometry. This represents an approximation to the experimental transition energy at the band maximum. In the DFT/SCI calculations the VDZd basis sets were augmented by one set of diffuse sp functions with $\alpha_{sp} = 0.06$, placed at the carbon and nitrogen atoms, which accounts for the lowest members of the Rydberg series and for the increased spatial extent of the higher-lying valence states.

In the SCI approach the singlet or triplet configuration state functions (CSF) resulting from the distribution of all valence electrons in all virtual MOs were included. All transition moments were calculated in the dipole length form.

Our initial interpretation of the experimental data[30,31] was based on semiempirical ZINDO calculations, and these results are presented in one of the tables for comparison. However, the precision of these results was not sufficient for an unambiguous assignment of the observed transitions.

## Results

The EEL spectra are shown and compared to the results of the DFT/SCI calculations in Figures 1−4. The experimental and calculated transition energies, the calculated dipole moments and oscillator strengths, and the approximate description of the transitions in terms of the MO configurations are summarized in Tables 1−4. Figure 5 defines labels of the benzene p orbitals, which are then used in the Tables 1−4 to designate MOs localized mainly on the benzene moiety.

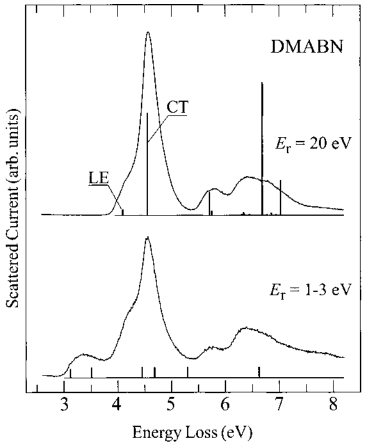

**Figure 1.** EEL spectra of DMABN. Vertical bars under the spectra indicate results of DFT/SCI calculations. Bar lengths are proportional to the calculated oscillator strengths for the singlet transitions.

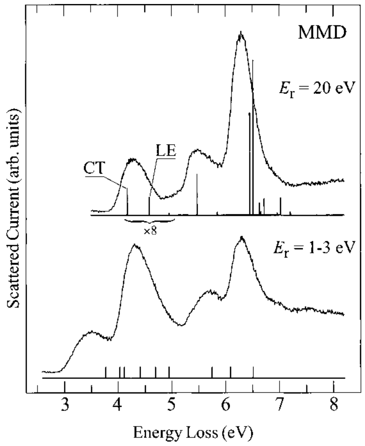

**Figure 2.** EEL spectra of MMD. Vertical bars indicate results of the DFT/SCI calculations (see caption of Figure 1). The lowest three vertical bars under the singlet spectrum are expanded for clarity.

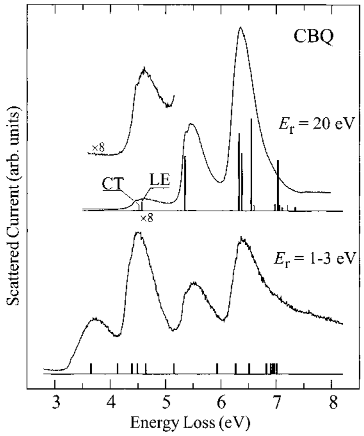

**Figure 3.** EEL spectra of CBQ. Vertical bars indicate results of the DFT/SCI calculations (see caption of Figure 1). The bar of the lowest LE transition is shown 8× vertically expanded. Transitions with oscillator strengths smaller than 0.001 (e.g., the lowest CT transition) are indicated by thinner bars.

**DMABN.** Five features can be distinguished in the high residual energy spectrum in Figure 1. The general shape of the spectrum and the magnitude of the transition energies agree well with the UV spectrum measured in isooctane and with the linear dichroism spectrum measured in polymer matrices by Herbich et al.[40] The energy gap between the $1^1B$ and $2^1A$ transitions is smaller in solution than in the gas phase and decreases with

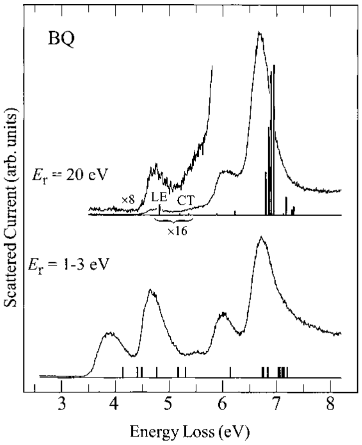

**Figure 4.** EEL spectra of BQ. Vertical bars indicate results of the DFT/SCI calculations (see caption of Figure 1). The lowest three vertical bars under the singlet spectrum are expanded for clarity.

**TABLE 1: Transition Energies of DMABN (in eV)[a]**

| | DFT/SCI | | | | |
|---|---|---|---|---|---|
| $\Delta E_{exp}$ | $\Delta E$ | $f \times$ 1000 | $\mu$ | state | assignment |
| | | | Singlets | | |
| 4.25 | 4.09 | 31 | 11.4 | $1B_2$ | $(p_N \rightarrow \pi_4) + (\pi_2 \rightarrow \pi_3)$ |
| 4.56 | 4.55 | 680 | 14.6 | $2A_1$ | $(p_N \rightarrow \pi_3)$ (CT) |
| 5.80 | 5.71 | 150 | 10.5 | $2B_2$ | $(\pi_2 \rightarrow \pi_3) + (\pi_1 \rightarrow \pi_4) - (\pi_2 \rightarrow \pi_4)$ |
| | 5.75 | 23 | 1.6 | $1B_1$ | $(p_N \rightarrow 3s)$ |
| | 6.31 | 0 | 19.3 | $1A_2$ | $(p_N \rightarrow 3p_y) + (p_N \rightarrow \pi^*_{CN})$ |
| | 6.34 | 11 | 10.1 | $3A_1$ | $(\pi_1 \rightarrow \pi_3)$ |
| | 6.36 | 0 | 2.9 | $2B_1$ | $(p_N \rightarrow 3p_z)$ |
| | 6.45 | 0 | 6.5 | $2A_2$ | $(p_N \rightarrow 3p_y) - (p_N \rightarrow \pi^*_{CN})$ |
| 6.40 | 6.69 | 890 | 8.0 | $4A_1$ | $(\pi_2 \rightarrow \pi_4)$ (benzene $E_{1u}$, z pol) |
| | 6.78 | 1 | 0.8 | $3B_1$ | $(p_N \rightarrow 3d_{x^2-y^2})$ |
| | 6.86 | 10 | 4.0 | $4B_1$ | $(p_N \rightarrow 3d_{z_2})$ |
| | 6.95 | 0 | 2.6 | $3A_2$ | $(\pi_{CN} \rightarrow \pi_3)$ |
| 6.80 | 7.03 | 230 | 8.4 | $3B_2$ | $(\pi_1 \rightarrow \pi_4) - (\pi_2 \rightarrow \pi_3)$ |
| | 7.10 | 0 | 2.7 | $4A_2$ | - |
| | 7.16 | 1 | 0.2 | $5A_1$ | $(p_N \rightarrow 3p_x)$ |
| | | | Triplets | | |
| 3.36 | 3.12 | | 14.0 | $1A_1$ | $(p_N \rightarrow \pi_3)$ |
| (3.5) | 3.51 | | 12.0 | $1B_2$ | $(p_N \rightarrow \pi_4)$ (mostly LE) |
| | 4.45 | | 8.1 | $2A_1$ | $(\pi_2 \rightarrow \pi_4)$ (benzene $E_{1u}$) |
| | 4.68 | | 10.3 | $2B_2$ | $(\pi_2 \rightarrow \pi_3)$ |

[a] Given are the experimental vertical ($\Delta E_{exp}$) transition energies (with an uncertainty of ±0.1 eV, except where otherwise noted), the theoretical vertical transition energies $\Delta E$, the oscillator strengths $f$, and the dipole moments $\mu$ (D). The symbols $\pi_1 - \pi_4$ in the "assignment" column designate those MOs of DMABN that are localized predominantly on the benzene ring and thus resemble the benzene MOs shown schematically in Figure 5 (the lowest benzene $\pi$-MO is labeled $\pi_0$). Orbitals consisting predominantly of the nitrogen lone pair and of the $\pi^*$ orbital of the CN moiety are labeled as $p_N$ and $\pi^*_{CN}$, respectively

**TABLE 2: Transition Energies of MMD (See Caption of Table 1)**

| | DFT/SCI | | | | |
|---|---|---|---|---|---|
| $\Delta E_{exp}$ | $\Delta E$ | $f \times$ 1000 | $\mu$ | state | assignment |
| | | | Singlets | | |
| 4.27 | 4.17 | 19 | 19.0 | 2A | $(p_N \rightarrow \pi_3)$ (CT) |
| | 4.58 | 13 | 7.8 | 3A | $(\pi_1 \rightarrow \pi_3) + (p_N \rightarrow \pi_4)$ (LE) |
| 5.0 | 4.95 | 2 | 17.2 | 4A | $(p_N \rightarrow \pi_4)$ (CT) |
| 5.45 | 5.47 | 231 | 8.7 | 5A | $(\pi_1 \rightarrow \pi_3) + (\pi_2 \rightarrow \pi_3)$ |
| | 5.85 | 17 | 4.7 | 6A | $(p_N \rightarrow 3s)$ |
| 6.30 | 6.45 | 577 | 7.4 | 7A | $(\pi_1/\pi_2 \rightarrow \pi_3/\pi_4)$ (benzene $E_{1u}$) |
| | 6.51 | 876 | 6.5 | 8A | $(\pi_1/\pi_2 \rightarrow \pi_3/\pi_4)$ (benzene $E_{1u}$) |
| | 6.63 | 68 | 7.7 | 9A | $(p_N \rightarrow 3p)$ + valence |
| | 6.66 | 18 | 10.3 | 10A | $(p_N \rightarrow 3p)$ + valence |
| | 6.72 | 92 | 6.6 | 11A | $(p_N \rightarrow 3p)$ + valence |
| | 6.93 | 3 | 5.4 | 12A | $(\pi_{CN} \rightarrow \pi_3)$ |
| | 6.96 | 13 | 16.2 | 13A | $p_N \rightarrow$ val. + Ryd. MOs |
| | 7.02 | 99 | 4.8 | 14A | $(\pi_0 \rightarrow \pi_3)$ |
| | 7.20 | 18 | 7.1 | 15A | $p_N \rightarrow$ val. + Ryd. MOs |
| | 7.21 | 9 | 2.5 | 16A | $(p_N \rightarrow \pi^*_{CN})$ |
| | | | Triplets | | |
| 3.48 | 3.77 | | 10.8 | 1A | $(\pi_2 \rightarrow \pi_3) + (p_N \rightarrow \pi_3) + (\pi_1 \rightarrow \pi_3)$ |
| 4.31 | 4.03 | | 8.2 | 2A | $(\pi_1 \rightarrow \pi_3) - (\pi_2 \rightarrow \pi_3)$ |
| | 4.11 | | 16.7 | 3A | $(p_N \rightarrow \pi_3)$ (CT) |
| | 4.41 | | 5.74 | 4A | $(\pi_1 \rightarrow \pi_4)$ |
| | 4.69 | | 11.6 | 5A | $(p_N \rightarrow \pi_4) + (\pi_2 \rightarrow \pi_4)$ |
| | 4.94 | | 11.9 | 6A | $(p_N \rightarrow \pi_4) - (\pi_2 \rightarrow \pi_4)$ |
| | 5.75 | | 4.0 | 7A | $(p_N \rightarrow 3s)$ |
| | 6.09 | | 5.1 | 8A | $(\pi_0 \rightarrow \pi_3)$ |
| | 6.51 | | 6.5 | 9A | |

**TABLE 3: Transition Energies of CBQ (See Caption of Table 1)**

| | DFT/SCI | | | | |
|---|---|---|---|---|---|
| $\Delta E_{exp}$ | $\Delta E$ | $f \times$ 1000 | $\mu$ | state | assignment |
| | | | Singlets | | |
| 4.60 | 4.52 | 0 | 20.0 | 1A″ | $(p_N \rightarrow \pi_3)$ ("TICT") |
| | 4.57 | 7 | 6.1 | 2A′ | $(\pi_1 \rightarrow \pi_3) + (\pi_2 \rightarrow \pi_4)$ ($L_b$) |
| 5.46 | 5.35 | 308 | 7.9 | 3A′ | $(\pi_2 \rightarrow \pi_3)$ |
| 6.35 | 6.33 | 438 | 6.1 | 4A′ | $(\pi_2 \rightarrow \pi_4) - (\pi_1 \rightarrow \pi_3)$ |
| | 6.38 | 326 | 5.0 | 5A′ | $(p_N \rightarrow 3s)$ + valence |
| | 6.55 | 522 | 5.9 | 6A′ | $(\pi_1 \rightarrow \pi_4) + (\pi_{CN} \rightarrow \pi_3)$ |
| | 6.60 | 0 | 11.9 | 2A″ | $(\sigma \rightarrow \pi_3)$ |
| | 6.98 | 38 | 6.3 | 7A′ | $(p_N \rightarrow 3p_z)$ |
| | 7.03 | 288 | 4.5 | 8A′ | $(\pi_{CN} \rightarrow \pi_3) - (\pi_1 \rightarrow \pi_4)$ |
| | 7.06 | 1 | 16.2 | 3A″ | |
| | 7.06 | 1 | 16.2 | 4A″ | |
| | 7.11 | 19 | 9.3 | 9A′ | |
| | 7.21 | 1 | 2.8 | 5A″ | |
| | 7.25 | 2 | 6.1 | 6A″ | |
| | 7.34 | 22 | 21.0 | 10A′ | |
| | | | Triplets | | |
| 3.70 | 3.65 | | 6.9 | 1A′ | $(\pi_2 \rightarrow \pi_3)$ $L_a$ |
| | 4.13 | | 8.1 | 2A′ | $(\pi_1 \rightarrow \pi_3)$ $L_b$ |
| 4.49 | 4.39 | | 4.4 | 3A′ | $(\pi_2 \rightarrow \pi_4) - (\pi_1 \rightarrow \pi_4)$ |
| | 4.49 | | 20.1 | 1A″ | $(p_N \rightarrow \pi_3)$ (TICT) |
| | 4.64 | | 4.9 | 4A′ | $(\pi_2 \rightarrow \pi_4) - (\pi_1 \rightarrow \pi_4)$ |

increasing solvent polarity,[13] in line with the higher dipole moment of the upper state.

We base our assignment on the comparison with the transition energies and oscillator strengths from the DFT/SCI calculations (Table 1). The assignment of the two lowest excited states in relation to the DFT/SCI calculation has already been discussed in the recent publication of Parusel et al.[21] The most intense band centered at 4.56 eV is attributed to a transition to the $2^1A_1$ state, calculated at 4.55 eV. Excited states have mixed CT and locally excited (LE) character in the untwisted compound, but orbital analysis and the large calculated dipole moment of 14.6 D reveal that this transition is predominantly CT. A shoulder observed at 4.25 eV is assigned to a transition to the $1^1B_2$ state, calculated at 4.09 eV. Orbital assignment (Table 1) and a smaller calculated dipole moment of 11.4 D reveal a substantial LE contribution to this state, although the CT character increases upon twisting of the amino group.[21] The DFT/SCI calculations reproduce the observed transition energies to remarkable accuracy. The calculated oscillator strength of the band at 4.09 eV is less than could be expected from the relative intensity of the 4.25 eV shoulder in the spectrum. We ascribe the higher experimental intensity to vibronic "intensity borrowing" from the transition to the higher-lying state, and possibly partly to deviation of the EEL intensities from the dipole transition

**TABLE 4: Transition Energies of BQ (See Caption of Table 1)**

| | DFT/SCI | | | | |
|---|---|---|---|---|---|
| $\Delta E_{exp}$ | $\Delta E$ | $f \times 1000$ | $\mu$ | state | assignment |
| | Singlets | | | | |
| 4.72 | 4.82 | 2 | 1.7 | 2A′ | |
| 5.52 | 5.20 | 0 | 12.1 | 1A″ | CT |
| | 5.37 | 0 | 12.6 | 2A″ | CT |
| 6.02 | 5.89 | 4 | 1.7 | 3A′ | LE |
| | 6.23 | 13 | 4.5 | 4A′ | LE |
| 6.70 | 6.80 | 170 | 2.2 | 5A′ | |
| | 6.86 | 353 | 3.6 | 6A′ | |
| | 6.90 | 577 | 0.2 | 7A′ | |
| | 6.92 | 0 | 5.7 | 3A″ | |
| | 6.95 | 605 | 2.3 | 8A′ | |
| | 7.13 | 2 | 5.4 | | |
| | 7.18 | 69 | 16.1 | | |
| | 7.18 | 18 | 2.8 | | |
| | 7.29 | 17 | 1.5 | | |
| | 7.32 | 29 | 4.1 | | |
| | Triplets | | | | |
| 3.88 | 4.14 | | 1.9 | 1A′ | |
| 4.67 | 4.41 | | 1.9 | 2A′ | |
| | 4.49 | | 1.6 | 3A′ | |
| | 4.77 | | 1.6 | 4A′ | |

**TABLE 5: Comparison of Experimental and Calculated Transition Energies (eV) of DMABN**

| state | exptl[a] | UV[b] | CNDO[c] | ZINDO[d] | CASPT2[e] | DFT/SCI[a] |
|---|---|---|---|---|---|---|
| $1^1B$ | 4.25 | (4.1) | 4.2 | 4.22 | 4.02 | 4.09 |
| $2^1A$ | 4.56 | 4.43 | 4.8 | 4.53 | 4.23 | 4.55 |
| $2^1B$ | 5.80 | | | 5.92 | | 5.75 |
| $4^1A$ | 6.40 | | | 6.40 | | 6.34 |
| $1^3A$ | 3.36 | | | 2.06 | 3.50 | 3.12 |
| $1^3B$ | (3.5) | | | 3.34 | 3.80 | 3.51 |

[a] Present work. [b] Reference 13, in *n*-heptane. The transition to the $1^1B$ state is seen as a shoulder on the band due to the transition to the $2^1A$ state, and its vertical energy cannot be determined reliably. [c] Reference 45. [d] References 30 and 31. [e] Reference 14.

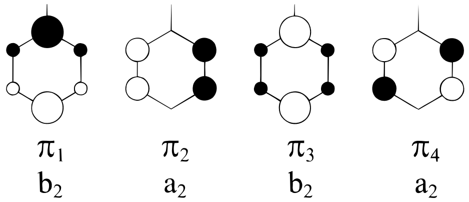

**Figure 5.** Definition of the labels of the high-lying occupied and the low-lying unoccupied MO's of benzene. The vertical line indicates the bond to the N atom. (The lowest-lying $\pi$-MO of benzene is not shown. It is denoted as $\pi_0$ in the tables).

moments at the comparatively low incident electron energies used in the present experiment. The situation is analogous to that found for the lowest singlet transition in benzene, which is well visible in the optical absorption and the EEL[27] spectra despite its zero oscillator strength with $D_{6h}$ symmetry.

Our assignment of the two lowest vertical excited states agrees with that of Herbich et al.[40] (based on INDO results) and with our earlier assignment[30,31] based on ZINDO calculations. Our assessment of the singlet states of DMABN is similar to that proposed by Köhler et al.[41] Table 5 compares our results of these two states with earlier experimental and theoretical work. (A more comprehensive list of previous calculations is given in refs 14, 20, and 21.) Figure 1 and Table 1 further indicate that the DFT/SCI calculation successfully accounts for even the higher excited states.

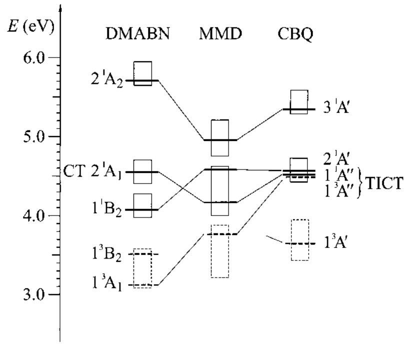

**Figure 6.** Correlation between observed spectral bands and calculated transition energies. Only the bands due to transitions to the lowest-lying one or two triplet states are shown. Spectral bands are indicated by rectangles, calculated energies by horizontal lines. Singlet states are indicated with solid lines, triplet states with dashed lines.

Spin-forbidden transitions appear, together with the dipole-allowed ones, in the lower curve of Figure 1, which was recorded with low residual energies. The lowest triplet transition peaks at 3.36 eV, which is consistent with the value of 2.8 eV (band maximum) determined from the phosphorescence spectrum in ethanol at 77 K by Köhler et al.[41] when the mirror image relationship of the EEL and the phosphorescence spectra is taken into account. (The band onsets are at 3.0 eV for both the energy-loss and the phosphorescence spectra.) This agreement provides support to the conclusion of Köhler et al.[41] that the phosphorescing species is coplanar. Comparison with theory (Table 1) assigns the first triplet band as ${}^3A_1$, in agreement with Köhler et al.[41] The calculation shows that it is a predominantly $p_N \rightarrow \pi_3$ transition, which means that it is related, in terms of orbital occupation, to the *second* (and not the first) excited singlet state of DMABN and to the TICT state of CBQ. The energy of this state is thus a very steep function of the twist angle (see also Figure 6). The SCI model is known to exaggerate excited-state dipole moments, and the dipole moment for the ${}^3A_1$ state indicated by our calculation is presumably too high. Our results thus do not contradict the conclusion of Köhler et al.[41] and Okada et al.[42] that the ${}^3A_1$ state in the coplanar conformation does not have substantial CT character. This is indicated by the fact that we calculate the dipole moments of the twisted CT states (the singlet and triplet 1A″ states of CBQ in Table 3) to be even much higher.

**MMD.** The spectrum measured with 20 eV residual energy shows three bands peaking at 4.27, 5.45, and 6.30 eV (Figure 2). The flat shape of the spectrum and the substantial magnitude of the signal in the 4.8−5.2 eV region indicate another transition around 5.0 eV. The EEL spectrum is similar to the UV spectra measured in isooctane[40] and in *n*-pentane.[13] The first UV absorption in the gas phase was reported at 4.3 eV.[35]

The lower symmetry of MMD compared to DMABN results in a larger mixing of different excited configurations, as indicated in Table 2. The lowest singlet transition is calculated to correspond to CT excitation. The second singlet excited state, a LE state, is calculated at 4.58 eV. This transition is calculated to have a small oscillator strength and is probably responsible in part for the broad 4.27 eV band. Note that this LE state, whose energy depends only to a small extent on the amino-group substitution pattern, becomes visible at about 4.4 eV in the photoabsorption spectrum of 3,5-dimethyl-4-aminobenzonitrile in *n*-pentane[13] where the CT state is strongly blue-shifted.

A weak transition is calculated at 4.95 eV and explains the signal at 5.0 eV. A locally excited state calculated at 5.47 eV accounts for the band at 5.45 eV. Finally, two intense transitions calculated at 6.45 and 6.51 eV (closely related to the strong $E_{1u}$ transitions of benzene) explain well the 6.30 eV band.

**TABLE 6: Comparison of Experimental and Calculated Transition Energies (eV) of CBQ**

| state | exptl[a] | UV[b] | ZINDO[c] | DFT/SCI[a] |
|---|---|---|---|---|
| $1^1A''$ (TICT) | (4.6) | (4.2) | 5.57 | 4.52 |
| $2^1A'$ | 4.60 | 4.60 | 4.32 | 4.57 |
| $3^1A'$ | 5.46 | | 4.96 | 5.35 |
| $2^3A'$ | 3.70 | | 2.79 | 3.65 |

[a] Present work. [b] Reference 44, in isooctane or methanol. The "TICT" band is observed only in acetonitrile. [c] References 30 and 31.

The onset of the first triplet band is very gradual, at about 3.0 eV in Figure 2, in agreement with the onset of the phosphorescence band observed at 2.9 eV[41] in glassy ethanolic solution (both at 77 K). The large relative intensity of the 4.31 eV band in the low $E_r$ spectrum, in comparison with the $E_r$ = 20 eV spectrum (Figure 2), indicates singlet−triplet transitions at this energy. An unambiguous assignment is not possible because four such transitions are calculated near this energy.

The calculated singlet−triplet (S−T) separation of the CT states in MMD is 0.06 eV, i.e., much less than in DMABN (1.4 eV). This trend may be understood as an indication of a more complete charge separation at larger twist angle, the limit of this trend being found in CBQ where the S−T separation nearly vanishes.

**CBQ.** CBQ exhibits a 90° twist angle of the amino group. The oscillator strength of the CT transition becomes very small, and it is no longer prominent in the $E_r$ = 20 eV spectrum. This situation is reflected in the spectra already on a qualitative level, since the $E_r$ = 20 eV spectrum is reminescent of the (slightly red-shifted) spectrum of benzene.[26,27] The intense CT bands found at low-energy loss in DMABN and with less intensity in MMD are now missing.

In the case of CBQ, the state with a perpendicularly twisted amino nitrogen (called "TICT" here in an extension of the normal usage)[43] is calculated to be the lowest singlet excited state with an oscillator strength of nearly zero. Since the lowest LE state is calculated to be only 0.05 eV higher, the TICT state cannot be distinguished as a separate band in the spectrum. The 4.60 eV band is probably due to both transitions and may derive a large part of its intensity from borrowing. This band overlap is somewhat disappointing given our initial hope that the less stringent selection rules of EEL spectroscopy will permit a direct observation of this unrelaxed TICT state.

The EEL transition energy for the first band is in excellent agreement with the photoabsorption value in isooctane or methanol[44] (Table 6). Both the EEL and the UV spectra show weak vibrational structure. The UV spectrum recorded in the polar solvent acetonitrile shows an additional weaker shoulder on the low-energy side of the 2A′ band, which was assigned to a transition to the TICT state by Rotkiewicz et al.[44] The absence of this feature in the present gas-phase spectra (see the expanded trace in Figure 3) indicates that selective stabilization of the CT state by polar solvents is required to make it visible as a separate spectral feature.

The onset of the first triplet band is at 3.25 eV in Figure 3, in very good agreement with the position of the 0−0 transition of the phosphorescence band observed at 3.35 eV[44] in *n*-propanol and at 3.3 eV[41] in glassy ethanolic solution (both at 77 K).

The DFT/SCI calculations also account very well for the higher-lying bands in the $E_r$ = 20 eV spectrum. The strongly enhanced relative intensity of the 4.49 eV band in the lower spectrum of Figure 3 indicates the appearance of triplet states that are assigned to the three overlapping transitions in Table 3 (one of them being the triplet TICT state).

**BQ.** BQ was investigated in order to determine the effect of the cyano group in CBQ. The spectrum at 20 eV residual energy is again reminiscent of the spectrum of benzene. Furthermore, it agrees with the DFT/SCI calculations when intensity enhancement of the low-lying bands by vibronic coupling is taken into account. The calculated dipole moments in Table 4 indicate that the lowest singlet state is of LE nature, emphasizing the need of the TICT state to be stabilized by the cyano group. The calculated dipole moments indicate two CT states at 5.20 and 5.37 eV that can be assigned to the shoulder at 5.52 eV. In contrast to CBQ, this state thus appears to give rise to a distinct CT band in BQ.

Finally, two triplet transitions at 3.88 and 4.67 eV can be distinguished in the spectrum measured at low residual energies.

## Discussion and Conclusions

An intriguing aspect of the research on DMABN and related compounds is that three models have been proposed to explain the dual fluorescence, and the question of which is correct has not yet been settled.[17,19,21] These models assume different configurations of the amino group in the relaxed fluorescing CT state of DMABN relative to the benzonitrile plane: perpendicular (TICT)[3], planar (WICT),[16,17] or the cyano substituent being in-plane bent (RICT).[15]

We emphasize that the present work cannot resolve this problem primarily because electron energy loss spectroscopy deals with isolated molecules in the gas phase and is limited to vertical transitions, whereas the anomalous dual fluorescence is intimately associated with solvation in solutions and requires substantial rearrangement of the nuclei, which represents a dramatic departure from the vertical excitation region.

The present paper makes an indirect contribution to this issue, however, by characterizing the gas-phase spectroscopy of the relevant chromophore for varying twist and pyramidalization angles of the amino group. The primary result is thus a test of the predictive power of theory. The test is very thorough because (i) both singlet and triplet excited states are tested, (ii) it includes high-lying excited states, and (iii) it is made for three compounds with widely varying ground-state twist and pyramidalization angles.

The results are summarized in the correlation diagram in Figure 6. The very good agreement of theory and experiment justifies confidence that the DFT/SCI model is able to predict correct excitation energies for widely varying configurations of the nuclei. The spectroscopic study reported here thus increases the weight of the conclusions reached on the properties of the potential surface of DMABN in ref 21, in which the same theoretical model is used. The present EEL spectra can be used to test future theoretical models.

The correlation diagram in Figure 6 further allows two more specific conclusions. The combined EELS and theoretical results indicate that the singlet $2A_1$ CT state of DMABN reached by a vertical transition in the gas phase is stabilized and becomes the lowest singlet state in MMD under these conditions. This result supports the conclusion of Parusel et al.[21] that in their gas-phase calculations the potential minimum of the CT state of DMABN is around 60° twist angle, near the ground-state twist angle of MMD. (The potential is very flat with both CASPT2[46] and DFT/SCI[21] methods, and it is not surprising that the exact position of the shallow minimum varies with different models; i.e., CASPT2 gives 45°, and DFT/SCI gives 60°.) The $2A_1$ CT state of DMABN is not further lowered but in contrast destabilized when the twist angle is further increased to 90° when going from MMD to CBQ. Since the calculation[21] indicates only a weak destabilization of this state when the twist angle is increased toward 90° in DMABN, we propose that the destabilization in CBQ is caused primarily by the large pyramidalization angle of the amino group found in this compound. To test this hypothesis we calculated the excitation energies of DMABN with 90° twist angle and a pyramidalization identical to that prevailing in CBQ and found 4.62 eV for the $L_b$ state and 4.88 eV for the "TICT" state. These values lie very close to 4.57 and 4.54 eV calculated for CBQ (Table 3). Theory thus suggests that the CT excited state is destabilized by the large pyramidalization angle in CBQ.

Finally, the present paper also characterizes the triplet states and indicates that the lowest triplet state of CBQ is not of CT type and differs substantially in terms of orbital occupation from the lowest triplet states of DMABN and MMD.

**Acknowledgment.** This work is part of Project No. 20-53568.98 of the Swiss National Science Foundation. The services and the computer time made available by the "Sonderforschungsbereich 334" ("Wechselwirkungen in Molekülen") of the "Deutsche Forschungsgemeinschaft" have been essential to this work.

## References and Notes

(1) Lippert, E.; Lüder, W.; Boos, H. In *Advances in Molecular Spectroscopy*, European Conference on Molecular Spectroscopy, Bologna, Italy, 1959; Mangini, A., Ed.; Pergamon: Oxford, 1962; p 443. (b) Lippert, E.; Lüder, W.; Moll, F.; Nägele, W.; Boos, H.; Prigge, H.; Seibold-Blankenstein, I. *Angew. Chem.* **1961**, *73*, 695.

(2) Rotkiewicz, K.; Grellmann, K. H.; Grabowski, Z. R. *Chem. Phys. Lett.* **1973**, *19*, 315. Erratum: *Chem. Phys. Lett.* **1973**, *21*, 212.

(3) Grabowski, Z. R.; Rotkiewicz, K.; Siemiarczuk, A.; Cowley, D. A.; Baumann, W. *Nouv. J. Chim.* **1979**, *3*, 443.

(4) Baumann, W.; Bischof, H.; Fröhling, J.-C.; Brittinger, C.; Rettig, W.; Rotkiewicz, K. *J. Photochem. Photobiol., A* **1992**, *64*, 49.

(5) Schuddeboom, W.; Jonker, S. A.; Warman, J.; Leinhos, U.; Kühnle, W.; Zachariasse, K. A. *J. Phys. Chem.* **1992**, *96*, 10809.

(6) Bischof, H.; Baumann, W.; Detzer, N.; Rotkiewicz, K. *Chem. Phys. Lett.* **1985**, *116*, 180.

(7) Suppan, P. *J. Lumin.* **1985**, *33*, 29.

(8) Suppan, P. *Chem. Phys. Lett.* **1986**, *128*, 160.

(9) Ghoneim, N.; Suppan, P. *Pure Appl. Chem.* **1993**, *65*, 1739.

(10) Bischof, H.; Baumann, W.; Detzer, N. *Chem. Phys. Lett.* **1985**, *116*, 180.

(11) Rettig, W. *Angew. Chem.* **1986**, *98*, 969.

(12) Rettig, W. *Top. Curr. Chem.* **1994**, *169*, 253.

(13) Zachariasse, K. A.; von der Haar, T.; Hebecker, A.; Leinhos, U.; Kühnle, W. *Pure Appl. Chem.* **1993**, *65*, 1745.

(14) Serrano-Andrés, L.; Merchán, M.; Roos, B. O.; Lindth, R. *J. Am. Chem. Soc.* **1995**, *117*, 3189.

(15) Sobolewski, A. L.; Domcke, W. *Chem. Phys. Lett.* **1996**, *259*, 1.

(16) Zachariasse, K. A.; Grobys, M.; von der Haar, Th.; Hebecker, A.; Il'ichev, Yu. V.; Jiang, Y.-B.; Morawski, O.; Kühnle, W. *J. Photochem. Photobiol., A* **1996**, *102*, 59.

(17) Il'ichev, Yu. V.; Kühnle, W.; Zachariasse, K. A. *J. Phys. Chem. A* **1998**, *102*, 5670.

(18) Heine, A.; Herbst-Irmer, R.; Stalke, D.; Kühnle, W.; Zachariasse, K. A. *Acta Crystallogr.* **1994**, *B50*, 363.

(19) Zachariasse, K. A.; Grobys, M.; Tauer, E. *Chem. Phys. Lett.* **1997**, *274*, 372.

(20) Scholes, G. D.; Phillips, D.; Gould, I. R. *Chem. Phys. Lett.* **1997**, *266*, 521.

(21) Parusel, A. B. J.; Köhler, G.; Grimme, S. *J. Phys. Chem. A* **1998**, *102*, 6297.

(22) Rettig, W.; Gleiter, R. *J. Phys. Chem.* **1985**, *89*, 4676.

(23) Grimme, S. *Chem. Phys. Lett.* **1996**, *259*, 128.

(24) Bulliard, C.; Allan, M.; Smith, J. M.; Hrovat, D. A.; Borden, W. T.; Grimme, S. *Chem. Phys.* **1997**, *225*, 153.

(25) Huber, V.; Asmis, K.; Sergenton, A.-Ch.; Allan, M.; Grimme, S. *J. Phys. Chem. A* **1998**, *102*, 3524.

(26) Allan, M. *J. Electron Spectrosc. Relat. Phenom.* **1989**, *48*, 219.

(27) Allan, M. *Helv. Chim. Acta* **1982**, *65*, 2008.

(28) Asmis, K.; Allan, M. *J. Phys. B* **1997**, *30*, 1961.

(29) Asmis, K.; Allan, M. *J. Chem. Phys.* **1997**, *106*, 7044.

(30) Wirtz, G. Diploma Thesis, University of Fribourg, Switzerland, 1993.

(31) Bulliard, Ch. Ph.D. Thesis, University of Fribourg, Switzerland, 1994.

(32) Love, B.; Goodman, M. M. *Chem. Ind. (London)* **1967**, 2026 ff.

(33) Baumann, W.; Nagy, Z.; Reis, H.; Detzer, N. *Chem. Phys. Lett.* **1994**, *224*, 517.

(34) Meisenheimer, J.; Finn, O.; Schneider, W. *Ann.* **1920**, *420*, 219 ff.

(35) Ahlrichs, R.; Bär, M.; Häser, M.; Horn, H.; Kölmel, H. *Chem. Phys. Lett.* **1989**, *162*, 165.

(36) Treutler, O.; Ahlrichs, R. *J. Chem. Phys.* **1995**, *102*, 346.

(37) Becke, A. D. *J. Chem. Phys.* **1993**, *98*, 5648.

(38) Schäfer, A.; Horn, H.; Ahlrichs, R. *J. Chem. Phys.* **1992**, *97*, 2571.

(39) Kajimoto, O.; Yokoyama, H.; Ooshima, Y.; Endo, Y. *Chem. Phys. Lett.* **1991**, *179*, 455.

(40) Herbich, J.; Rotkiewicz, K.; Waluk, J.; Andresen, B.; Thulstrup, E. W. *Chem. Phys.* **1989**, *138*, 105.

(41) Köhler, G.; Grabner, G.; Rotkiewicz, K. *Chem. Phys.* **1993**, *173*, 275.

(42) Okada, T.; Uesugi, M.; Köhler, G.; Rechthaller, K.; Rotkiewicz, K.; Grabner, G. *Chem. Phys.* **1999**, *241*, 327.

(43) TICT refers here to a state reached by a vertical transition in the gas phase, with the amino group being twisted already in the ground state. The acronym TICT is thus used in a somewhat broader sense than is customary in the discussions of dual fluorescence, where it refers to a relaxed state in solution in which the amino group is electronically decoupled from the rest of the molecule by a twist of 90°.

(44) Rotkiewicz, K.; Rubaszewska, W. *Chem. Phys. Lett.* **1980**, *70*, 444.

(45) Rettig, W.; Bonaćić-Koutecký, V. *Chem. Phys. Lett.* **1979**, *62*, 115.

(46) Sobolewski, A. L.; Sudholt, W.; Domcke, W. *J. Phys. Chem.* **1998**, *102*, 2716.